JOURNAL OF GUIDANCE, CONTROL, AND DYNAMICS
Vol. 31, No. 1, January–February 2008

Nonlinear Attitude Control Laws for the Bell 412 Helicopter

Daniel J. Walker,* Mark Voskuijl,† and Binoy J. Manimala‡
University of Liverpool, Liverpool, England L69 7ZG, United Kingdom
and
Arthur W. Gubbels§
National Research Council of Canada, Ottawa, Ontario K1A 0R6, Canada

DOI: 10.2514/1.28945

Helicopters generally exhibit a ratelike response type in pitch and roll axes, and when feedback control is used to increase the level of augmentation to provide attitude command and attitude hold, there is generally a reduction in performance. Use of nonlinear elements in the control system can lead to recovery of some of this performance. The paper investigates such use of nonlinearities in the pitch control loop of a helicopter with a full-authority digital fly-by-wire control system. The nonlinear elements are used to specify the rate of response and thus the attitude quickness. Describing function analysis was used to test compliance with the relative stability requirements of MIL-F-9490D. The control laws were successfully flight-tested on a Bell 412 modified for fly-by-wire research and results from those tests are presented. Control laws of the type presented here can potentially be optimized to maximize agility within the available actuator limits. The first control law presented was intended to test the concept; modest pitch-axis performance was therefore specified. The second control law was designed to provide ADS-33E-PRF level-1 handling qualities for noncombat-mission task elements. Both controllers gave a stable closed loop and provided the required response type. Closed-loop bandwidth predictions based on analysis of linear models were close to the bandwidths achieved in flight. Likewise, the attitude quickness achieved in flight was very close to that specified via the nonlinear element.

Nomenclature

G	=	linear aircraft model
K	=	proportional gain, sector bound of nonlinearity
K_i	=	integral gain
K_q	=	pitch-rate gain
L	=	frequency response function
$N(a)$	=	describing function of a nonlinearity, function of amplitude
p	=	roll rate
Q_θ	=	pitch attitude quickness
Q_ϕ	=	roll attitude quickness
q	=	pitch rate
q_{ref}	=	internally generated pitch-rate reference
r	=	yaw rate
r_{dem}	=	demanded r
s	=	Laplace variable
X_B	=	longitudinal stick position
Θ, Θ_{trim}	=	pitch attitude, trim value
θ	=	pitch attitude perturbation about the trim
θ_{dem}	=	demanded θ
$\theta_{0,\text{tr}}$	=	tail rotor collective pitch angle
μ	=	real part of the root
τ_p	=	phase delay
Φ, Φ_{trim}	=	bank angle, trim value
ϕ	=	bank angle perturbation about the trim
ϕ_{dem}	=	demanded ϕ
ω	=	frequency
ω_{BW}	=	bandwidth

Received 20 December 2006; revision received 27 August 2007; accepted for publication 28 August 2007.

*Senior Lecturer, Engineering Department.
†Ph.D. Student, Engineering Department.
‡Research Associate, Engineering Department.
§Research Officer, Institute of Aerospace Research.

I. Introduction

THE introduction of active control technology makes the implementation of new and potentially better control laws possible, leading to higher performance, the ability to operate more safely, in worse conditions, and closer to the extremes of the flight envelope. The work presented in this paper was performed within the Helicopter Active Control Technology (HELIACT) project, which involves collaboration between the University of Liverpool and the National Research Council (NRC) of Canada. The project has had access to a six-axis motion-based flight simulator (HELIFLIGHT) at the University and a fly-by-wire (FBW) research Bell 412 helicopter at the NRC, the Advanced Systems Research Aircraft (ASRA) [1,2], shown in Fig. 1.

From the control law point of view, the focus of the project has been on developing methods for handling-quality improvement, active structural load alleviation, and envelope protection, concentrating on full-authority control, with the broad aim of investigating how the freedom that fly-by-wire affords can be exploited. A nonlinear simulation model [3] of the ASRA was created in the project and several control laws have been designed based on it and successfully flight-tested on the ASRA. The first successful flight test during the project was of a multivariable control law designed with the H_∞ loop-shaping design method [4]. This was the first test of such a controller on a high-performance hingeless-rotor helicopter. Other control laws tested were designed with classical techniques. These were all designed for the low-speed region of the flight envelope and provide an attitude-command/attitude-hold (ACAH) response type in the pitch and roll axes and a rate command (RC) response type in yaw.

The era of production rotorcraft with digital fly-by-wire control systems and task-tailored control laws started in 1989 with the V-22 Osprey tiltrotor [5]. ACAH control laws have been implemented on several helicopter types over the last decade. A recent example is the upgrade of the CH-47 Chinook with a digital flight control system [6]. This aircraft will be the first production helicopter of the U.S. Army that meets all the degraded environment response-type requirements defined in ADS-33E-PRF [7]. ACAH is one of the response types implemented on the Chinook digital flight control system. Another example is the upgrade of the UH-60 Black Hawk with modernized control laws, providing an ACAH response type

Fig. 1 National Research Council's Bell 412 Advanced Systems Research Aircraft.

[8]. The 10% authority stability augmentation system actuators on this aircraft were used to achieve this. By contrast, the results presented here relate to full-authority systems flight-tested on an experimental FBW helicopter.

Attitude quickness is a measure of the agility with which a rotorcraft can change its attitude or heading and partly defines the moderate-amplitude handling qualities. The pitch-attitude-quickness parameter is defined in ADS-33E-PRF [7], as in Eq. (1):

$$Q_\theta = \frac{q_{\text{pk}}}{\Delta\theta_{\text{pk}}} \tag{1}$$

where the subscript pk denotes the peak value reached during a maneuver following an abrupt step-attitude demand without significant reversals. The same document defines acceptable limits for this parameter. This paper shows how a nonlinear control element in a feedback loop can be combined with a linear control law to shape the speed of the response, such that a nonlinear ACAH response type with specified attitude quickness is achieved.

The first aim of the research was to develop a design process and related analysis tools for the development of control laws containing static nonlinear elements and to compare how the resulting system perform in flight on the ASRA compared with predictions based on new simulation models created in the project. The first task was to identify practical nonlinear stability analysis techniques. A conservative stability criterion would unnecessarily limit the performance of the system. The design process presented here has also been applied to the design of an envelope protection system for the mast torque on the ASRA and control laws, providing a translational rate command (TRC) response type. The TRC control laws use an ACAH inner-loop system, in which the attitude reference signal is based on a translational rate error. This attitude reference will have to be limited with a nonlinear element, because a large translational rate error could result in a very large attitude reference signal, which is undesirable.

The second aim of the research was to investigate whether handling qualities can be improved by providing an ACAH response type with a fixed speed of response. Four potential improvements can be identified. First, the method may potentially be used to maximize the agility while providing an ACAH response type. Second, the actuator usage is determined by the nonlinear element in the feedback loop. This can be useful when actuator saturation is an issue. Third, a fixed speed of response can be used as a means of harmonizing the response characteristics to inputs in the longitudinal and lateral axes. Control harmony is an important aspect of flying qualities [9]. Fourth, the method may be implemented in an autopilot to give the system smooth ride characteristics. Two controllers are presented in this paper. The first, designated FCL001, was designed to provide modest performance and was tested as a proof of concept. The second controller (FCL002) was designed to provide level-1-predicted handling qualities for all other MTEs, as defined in ADS-33E-PRF [7]. A distinction is made in ADS-33E-PRF between MTEs for which precise and aggressive maneuvering is required (typically combat maneuvers) and for MTEs that require moderate or limited agility. In this paper, the first set of MTEs is referred to as combat MTEs or target acquisition and tracking MTEs and the second set is referred to as all other MTEs. The handling-quality boundaries are defined separately for these two sets. The rest of the paper is organized as follows. The ASRA and the nonlinear simulation model are described in Sec. II. The two nonlinear flight control laws are described in Sec. III. These control laws are then subjected to an offline analysis (Sec. IV). Section V gives a description of the HELIFLIGHT flight simulator and the piloted simulation of the control laws. The flight tests are discussed in Sec. VI and Conclusions are in Sec. VII.

II. Bell 412 Advanced Systems Research Aircraft

The ASRA (Fig. 1) is a Bell 412, operated by the Canadian NRC [10] and extensively modified for use as an airborne simulator. It is equipped with a full-authority simplex control architecture with a single nonredundant set of FBW actuators, sensors, and flight control computer and software. The simplicity of the architecture facilitates the incorporation of software changes without the overhead of multiple coding sources, multiple languages or operating systems, and in-depth code validation. These overheads are necessary for production systems, but are overly prohibitive for flexible research programs. Inherent to the design philosophy of ASRA's simplex architecture is a reliance on automated safety monitoring systems (health monitoring unit) and a safety pilot to guard against system failure or operational flight envelope exceedance. This requires an increased reliance on the safety pilot and adds to his workload. However, the combination of the safety pilot and an automated safety monitoring system allows for FBW engaged flight throughout the entire certified operational flight envelope.

The ASRA control system structure (Fig. 2) consists of both safety pilot and evaluation pilot control paths. The safety pilot flies the helicopter using the certified mechanical control system and is responsible for assuming control in the event of a computer malfunction or other potentially dangerous situation. The evaluation pilot's controls, when engaged by the safety pilot, control the ASRA through a fully programmable, full-authority, fly-by-wire control system. The cyclic stick of the evaluation pilot is a center stick with a full throw of ± 6.5 in. laterally and longitudinally. This stick has a moderate force gradient for stick centering of approximately 1 lb/in. There was a small (0.1 in.) deadband around the center. The pedals were also a moderate gradient (approximately 2 lb/in.) with good centering characteristics. The range of the pedals is ± 3 in. The collective had no centering, but friction was equivalent to approximately 1 lb, enough to keep it in place if the pilot were to let go. The collective stick range is approximately 0–10 in. A wide range of flight parameters are measured and stored by the flight control computer at a data rate of 128 Hz. These parameters are available for use as feedback values in various aircraft control system schemes. Conventional parameters such as aircraft angular rates and attitudes are measured, as well as more unconventional parameters such as rotor flapping angles, angle of attack, and angle of sideslip. The high control power and bandwidth of the Bell 412 rotor system allow high-bandwidth flight control systems to be tested on the ASRA. The structure of the fly-by-wire system is such that new control laws can be implemented and tested rapidly. This makes the ASRA an ideal platform for research into novel control concepts.

A high-fidelity nonlinear simulation model of the Bell 412 ASRA has been developed previously within the HELIACT project [3]. The simulation program FLIGHTLAB [11] was used for this. The model, designated FB412, uses a rigid blade-element formulation of the

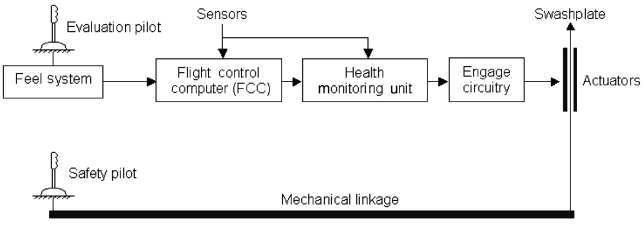

Fig. 2 Bell 412 ASRA control system structure schematic.

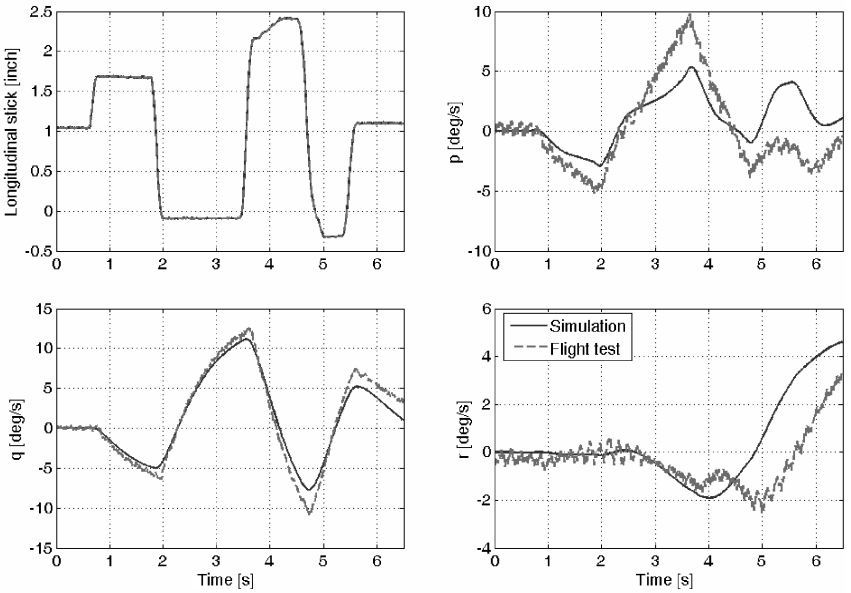

Fig. 3 Model validation: dynamic response due to a longitudinal input.

main rotor. The air loads acting on the blade elements are calculated with quasi-steady aerodynamics. The Peters–He [12] finite state inflow model was used. A Bailey [13] rotor model represents the tail rotor. Aerodynamic lookup tables represent all fuselage aerodynamics, the vertical fin, and the horizontal tail plane. The data required for the development of this model were partly acquired from the open literature and partly by measurements performed on the ASRA at the NRC Canada. The model was validated against a set of flight test data, and the main conclusion was that excellent correlation of the on-axis aircraft response was achieved between the nonlinear simulation model and the actual aircraft. However, the off-axis response correlation was not as good [3]. In parallel to this, linear models were also developed directly from flight test data using system identification. Figure 3 shows the dynamic response of the FB412 to a longitudinal stick input superimposed on that of the actual aircraft. This flight test was conducted at a 66-kt forward flight at a barometric altitude of approximately 3000 ft. The primary response (pitch rate q) is well-predicted; off-axis predictions (p and r) are less accurate, although the main characteristics are clearly captured.

Linear models were obtained by numerical perturbation of the FB412 nonlinear model. Sets of 9-state and 28-state linearizations were obtained over the range of 0–120 kt. The 9-state model consists of nine rigid-body states. The 28-state model consists of 9 rigid-body states, 16 rotor states (8 flap and 8 lag), and 3 rotor inflow states. The 9-state model is merely used to obtain a physical understanding of the system and the 28-state model is used for the actual control law design. Handling qualities are strongly influenced by the stability of the natural modes [9]. The eigenvalues of the 9-state linear models as a function of airspeed are presented in Fig. 4. The phugoidlike mode is unstable over most of the speed range; it is on the border of the level-3 region at hover. (Note that at low speed, the mode is somewhat different in nature from the phugoid mode of classical fixed-wing flight dynamics.) The Dutch roll mode is lightly damped: level 2 in terms of ADS-33E-PRF [7] requirements.

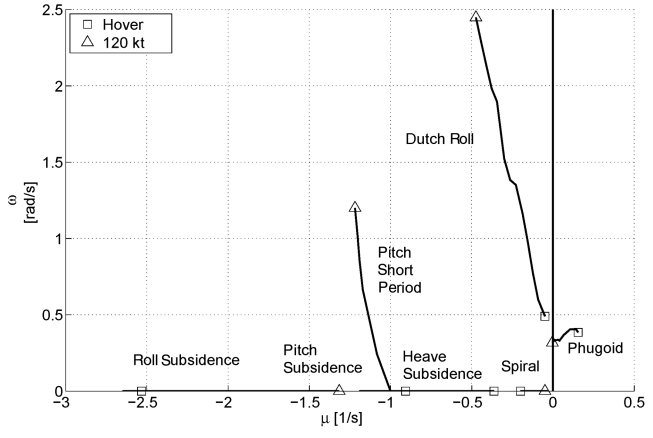

Fig. 4 Eigenvalue loci: FB412 model (unaugmented).

III. Nonlinear Control Law Design

The designs commenced with synthesis and analysis using the 28-state linear models in the MATLAB/SIMULINK environment. This was followed by nonlinear analysis and piloted simulation using FLIGHTLAB. The control laws were then discretised and coded into C for flight-testing. Two slightly different control architectures are presented, both designed to meet relevant criteria from ADS-33E-PRF. The first design carried out was to prove the concept; the second was tuned to provide higher performance. The designs were based on the 10-kt condition, because this would be challenging, owing to the stability and cross-coupling characteristics of the helicopter and to the significant changes in dynamics in that neighborhood [14].

A. Flight Control Law 1

FCL001 is a classical decoupled controller providing an ACAH response type in the pitch and roll axes and an RC response type in yaw; the heave axis was open loop. The pitch-axis control loop is shown in Fig. 5. The linear aircraft model in this figure is represented by $G(s)$. The gains K, K_i, and K_q were tuned to give an inner-loop bandwidth of 3.9 rad/s.

The inner loop provides a linear ACAH response type; it is fed by a pitch attitude reference generated by a cascaded integrator and a saturating nonlinear element. The latter can be used to define the speed of response and thus tailor the moderate amplitude characteristics of the vehicle. Note that pitch rate and attitude are mixed and fed back in the inner loop; this is broadly equivalent to

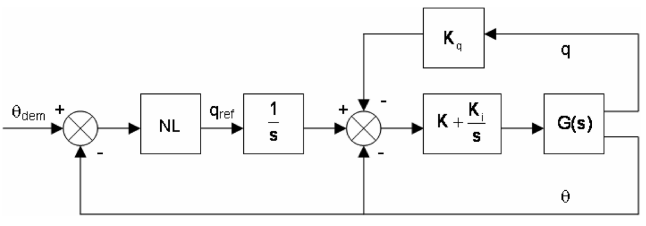

Fig. 5 Structure of the longitudinal subcontroller of FCL001.

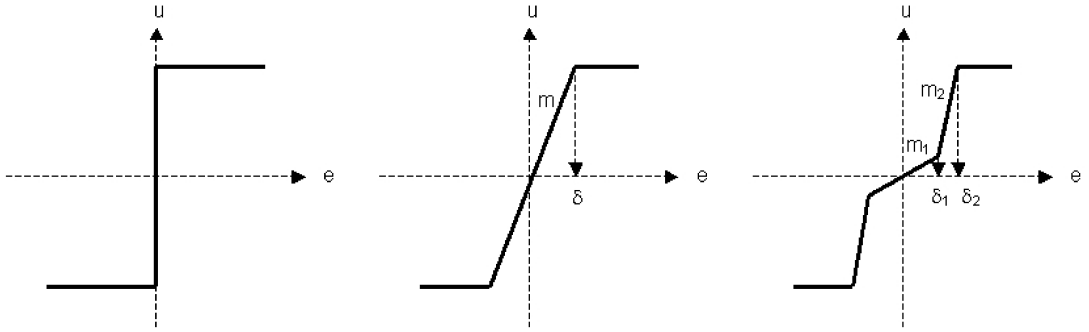

a) Relay b) Saturation c) Piecewise linear

Fig. 6 Nonlinear elements.

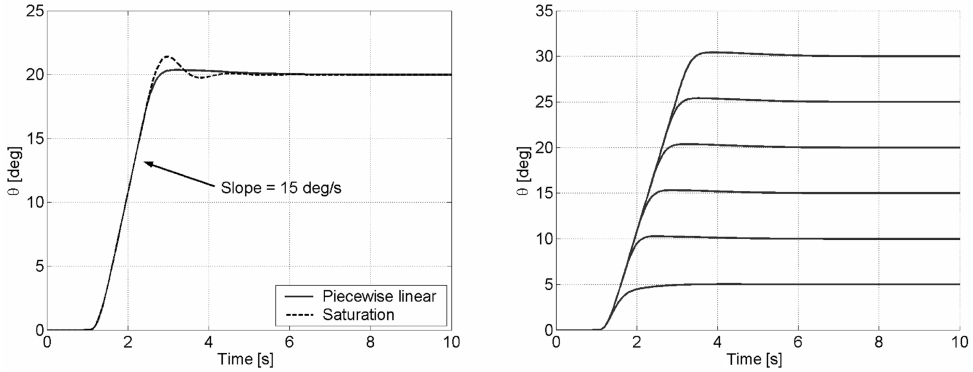

Fig. 7 Test of different types of nonlinearities at 10-kt forward flight in the linear domain (left) and different size step inputs with FCL001 with a piecewise-linear element (right).

using pitch attitude feedback and a proportional–integral–derivative control law, but it is less sensitive to noise. The roll and yaw loops used pure proportional–integral control. Three different nonlinear elements were considered: 1) relay, 2) saturation, and 3) piecewise linear (Fig. 6).

Without dead band, the relay will clearly give rise to a limit-cycle oscillation and was therefore discarded. The saturation gave a significant improvement; however, some overshoot was present (Fig. 7). The piecewise-linear element is similar to the saturation, but has smaller gain for small inputs. This gave the desired speed of response, with no perceptible overshoot. The response to different size step inputs is also shown in Fig. 7. Note how the speed of response is essentially fixed to 15 deg/s, regardless of the magnitude of the input. The overshoot in this linear simulation is minimal for all inputs.

B. Flight Control Law 2

FCL002 was designed to give the same response type as FCL001, but using an inner loop stabilized on pitch rate alone and providing an RC response type. FCL002's longitudinal controller structure is shown in Fig. 8. The linear aircraft model in this figure is represented by $G(s)$. The speed of response was again set to 15 deg/s. FCL002 was designed to give level-1 handling qualities for all other MTEs. The modified inner-loop control law allowed a higher bandwidth to be achieved, other things being equal. Roll, yaw, and collective control are identical to that of FCL001.

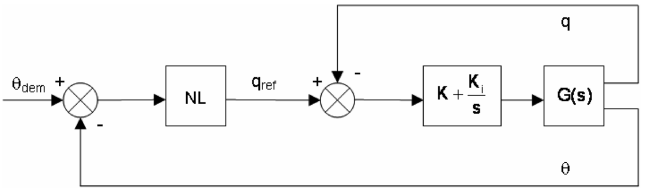

Fig. 8 Structure of the longitudinal subcontroller of FCL002.

IV. Offline Control Law Analysis

The control laws presented here both consist of an inner and an outer loop and a nonlinear element, and it is important to assess their stability and its robustness. When a linearized model $G(s)$ represents the flight dynamics, the inner-loop subsystems in Figs. 5 and 8 are linear. The robust stability requirements from MIL-F-9490D [15] were applied to determine whether the relative stability of the control law is satisfactory. Reference [16] shows that these requirements are more stringent than the disturbance rejection requirements specified in ADS-33E-PRF. According to MIL-F-9490D, gain and phase margins should be larger than 6 dB and 45 deg, respectively, at the frequencies of the rigid-body modes. These margins have to be met for the inner loop as well as the outer loop. To assess stability of the outer loop, both describing function analysis [17] and the Popov criterion [18] were applied.

A. Describing Function Analysis

Describing function analysis is a method for investigating the existence of limit cycles in nonlinear systems. It is an approximate technique; it can predict limit cycles that in practice do not exist or vice versa. Based on frequency-domain concepts and a simple graphical test, it has been widely used as an engineering tool for decades. Describing function analysis can be performed graphically with a polar plot. A limit cycle is predicted when the polar plot of G intersects with the plot of $-1/N$, where N is the describing function of the nonlinearity. Note that the nonlinear elements of FCL001 and FCL002 are not identical even though the rate of response is the same for both. The variables δ_1 and δ_2 are tuned to reduce overshoot. These are different for FCL001 and FCL002, which explains why the describing functions of both controllers differ in Figs. 9 and 10. This limit cycle can be either stable or unstable. Gain and phase margins can be calculated analogously to the purely linear case, as shown in Fig. 9; these indicate the distance to the limit cycle. The describing function analysis indicates outer-loop gain and phase margins of 11.1 dB and 56 deg, respectively, for FCL001; the corresponding

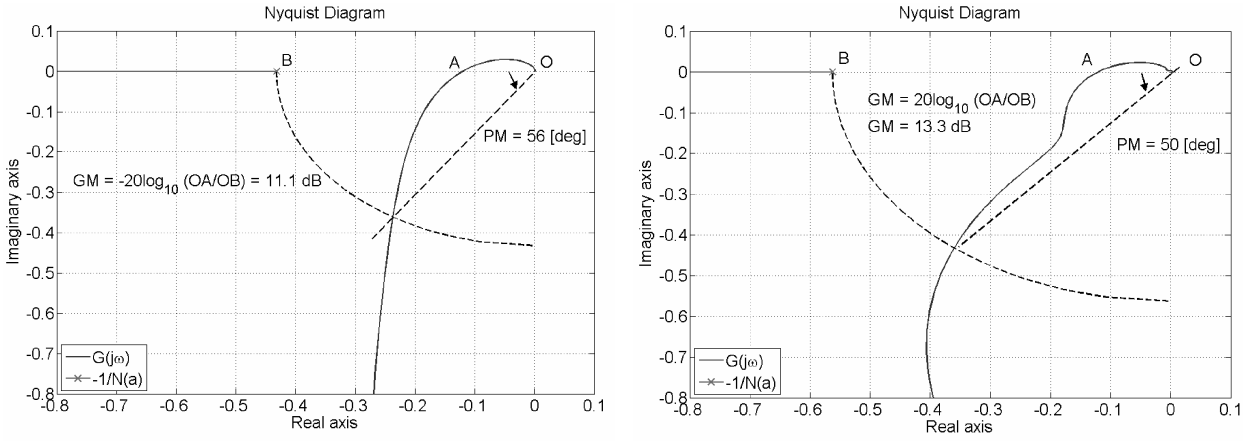

a) FCL001 **b) FCL001**

Fig. 9 Describing function analysis: pitch axis at 10 kt.

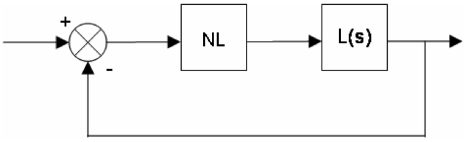

Fig. 10 Feedback loop containing memoryless nonlinear element NL.

values for FCL002 are 13.3 dB and 50 deg, respectively. This implies that the stability margins specified in MIL-F-9490D are achieved for the nonlinear outer loop of both controllers. The (nominally) linear roll and yaw loops of the controllers were analyzed with conventional techniques and it was found that the gain and phase margins in all axes complied with the requirements.

B. Popov Criterion

The Popov test provides a conservative test for the global asymptotic stability of a feedback system containing a linear time-invariant element with transfer function $L(s)$ and a sector-bounded static nonlinearity (NL in Fig. 10).

The criterion is met when the so-called modified frequency response $L^*(j\omega)$ defined in Eq. (2) lies to the right of a straight line passing through the point $-1/K$, where K is the sector bound of the nonlinearity, a so-called Popov line. There are no restrictions on the slope of the Popov line for the nonlinearities considered.

$$L^*(j\omega) = \mathrm{re}[L(j\omega)] + j\omega\,\mathrm{im}[L(j\omega)] \tag{2}$$

where $L(s)$ is the inner-loop transfer function from q_{ref} to θ in Figs. 5 and 8. The modified frequency response functions and Popov lines for FCL001 and FCL002 at the design condition are shown in Fig. 11. The sector bound K is slightly smaller for FCL002 even though both controllers have the same speed of response (15 deg/s). In addition to the speed of response, the sector bound depends on the variable δ_2 (Fig. 6c) as well. This variable was tuned to minimize overshoot and set to 7 deg for FCL002 and to 5 deg for FCL001. It can be concluded that the Popov criterion is met for both controllers and thus global asymptotic stability of the system is indicated at the design condition. As a conservative test, the Popov criterion gives sufficient conditions; that is, the feedback system is not necessarily unstable when the Popov criterion is not met. However, it is important to note that in practice, there will be nonlinearities in the inner-loop (aerodynamics, actuator limits, engine governor dynamics, and so on) that still have the potential to destabilize the system.

C. Predicted Attitude Quickness

The predicted handling qualities discussed in this section were calculated using the nonlinear simulation model. The parameter of main interest is the pitch attitude quickness, as defined in Eq. (1). For the designs proposed here, the speed of response ($q_{\max}$) is approximately constant, fixed by the nonlinearity, hence the attitude quickness will have a hyperbola ($1/x$) shape. Two cases are shown in Fig. 12: one with a 10 deg/s speed of response and the other with 15 deg/s. The speed of response can be increased until stability margin limits or the performance limits of the vehicle are reached. The pitch attitude quickness is well within the level-1 region for all other MTEs when the speed of response is set to 10 or 15 deg/s. Roll and yaw quickness of both controllers are also both in the level-1 region for all other MTEs.

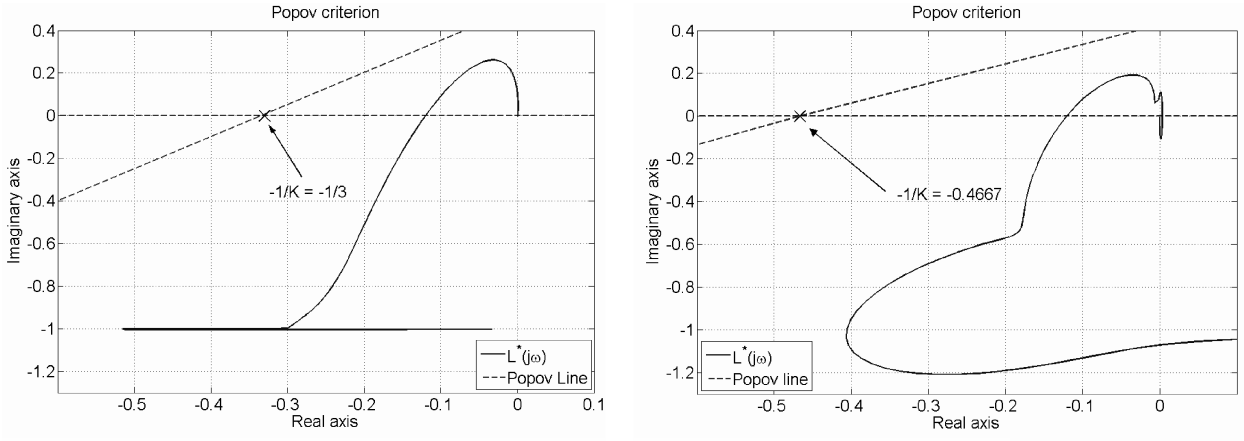

a) FCL001 **b) FCL002**

Fig. 11 Frequency response and Popov lines: pitch axis at 10 kt.

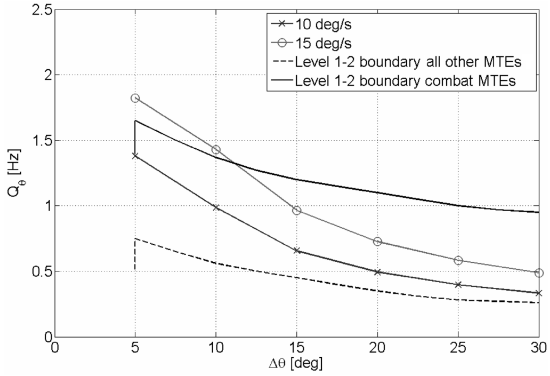

Fig. 12 Pitch attitude quickness at 10-kt forward flight.

D. Predicted Bandwidth and Phase Delay

The bandwidths and phase delays of both control laws were calculated in the manner specified in ADS-33E-PRF by applying frequency response analysis techniques to the 28-state linear model at the 10-kt design condition. The results are given in Table 1. A notable difference between FCL001 and FCL002 is the factor of 2.4 difference in the pitch-axis bandwidths; the modified structure of FCL002 allowed higher bandwidth while maintaining similar stability margins. All the bandwidths are level 1 for all other MTEs.

Finally, interaxis coupling criteria were checked. All criteria considered (pitch due to roll, roll due to pitch, and yaw due to collective) were found to be well within the level-1 region.

In summary, the predicted handling qualities of FCL001 are level 1 when all other MTEs are considered. The attitude quickness drops below the level-1–2 boundary for combat MTEs in all three axes. FCL002 has the same predicted handling qualities. The bandwidth in the pitch axis is much higher, well within the level-1 region for target acquisition and tracking MTEs

V. Piloted Simulation

The control law FCL001 was subjected to a piloted simulator trial in the HELIFLIGHT [19] simulator at the University of Liverpool. The aim was to test the system with a pilot in the loop. HELIFLIGHT is a reconfigurable flight simulator with the following five key components: 1) selective fidelity, aircraft-specific, interchangeable flight dynamics modeling software (FLIGHTLAB) with a real-time interface; 2) six-degree-of-freedom motion platform; 3) four-axis dynamic control loading; 4) three-channel collimated visual display for forward view, plus two flat-panel chin windows, providing a wide-field-of-view visual system, each channel running a visual database; and 5) reconfigurable computer-generated instrument display panel and head-up display.

HELIFLIGHT is used for piloted evaluation of aircraft models and flight systems in support of the Flight Science and Technology Research Group's activities.

The performance of the inner loop was set somewhat higher than described in Sec. III. The stability of the system in the real-time environment was first established. The following MTEs were selected: acceleration–deceleration, sidestep, slalom, and deck landing. Together, these allow the performance of the control law to be tested in all axes. A description of the first three MTEs can be found in ADS-33E-PRF [7]; the deck landing MTE is described in [20]. The Cooper–Harper handling-quality ratings (HQR) [21] obtained in the trial are summarized in Table 2.

Table 1 Bandwidths of FCL001 and FCL002 on the 28-state linear model at 10 kt

Controller	ω_{BW}, rad/s	τ_p, s	Predicted handling quality	
			Target acquisition and tracking MTEs	All other MTEs
FCL001 (pitch)	1.6	0.21	2	1
FCL002 (pitch)	3.9	0.7	1	1
FCL001 (roll)	4.2	0.7	1	1
FCL002 (roll)	4.1	0.7	1	1
FCL001 (yaw)	2.5	0.2	2	1
FCL002 (yaw)	2.4	0.2	2	1

Table 2 HQRs obtained in piloted simulation good visual environment (GVE) with FCL001 and a high-performance inner loop

ADS-33E-PRF mission task element	Cooper–Harper HQR
Sidestep	2
Acceleration–deceleration	4
Slalom	4
Deck landing	2

Both the sidestep and the acceleration–deceleration are relatively difficult maneuvers. The pilot stated that the limited field of view in the simulator was a factor in the higher (i.e., worse) HQR for the acceleration–deceleration MTE. The main difference between the sidestep maneuver and the acceleration–deceleration maneuver in terms of workload relates to torque monitoring, which is more of an issue in the acceleration–deceleration MTE. In the slalom maneuver, a fair amount of pedal was required while turning, because the control law provided a rate command response type in yaw; the workload would be reduced by the introduction of a turn-coordination system.

The simulated deck landing MTE was performed on a stationary type-23 frigate in zero-wind conditions and without ship motion due to waves. The purpose of the trial was primarily to investigate the pitch control law, which included the nonlinear element. The pitch rate was set to 15 deg/s because the pilot indicated that such agility was necessary for these MTEs. The pilot commented that a constant speed of response was pleasant because it made the aircraft behavior in pitch very predictable. The conclusion from this trial was that this type of control law was worth testing in flight, as part of the process of confidence-building in the wider modeling and control project.

VI. Flight Test of the Control Laws

In June 2006, a flight test of FCL001 was performed on the NRC Bell 412 ASRA, during which the control law was tested and data recorded. A similar flight test was performed with FCL002 in October 2006. Before describing the tests, we first briefly describe something of the control law implementation. First, the controller dynamics were discretized using a zero-order hold. The equations were then hand-coded in C and embedded in the flight control computer of the aircraft. The control law equations were derived on the basis of small perturbation models, and because neither the feedback signals Θ, Φ, P, Q, and R nor the stick positions will generally be zero upon engagement of the controller, it is necessary to account properly for the trim offsets. The C program contains an initialization subroutine that captures and stores the attitude, rate, and stick positions at the moment of engagement; these are subsequently treated as trim offsets to be subtracted from sampled measurements to produce the perturbation terms (θ, ϕ, p, q, r, etc.) that drive the control law dynamics. The pitch and roll attitude demands and the yaw rate demand are produced by multiplying the appropriate stick or pedal perturbation by a control gearing (Table 3), as in Eq. (3):

$$\theta_{\text{dem}} = (X_B - X_{B,\text{trim}}) \times \text{stick gearing} \tag{3}$$

A. Flight Test of FCL001

FCL001 was tested at approximately 20 kt, close to the design condition of 10 kt. Upon engagement, it was found that the closed-loop system was stable. Two portions of data for the pitch axis are shown in Figs. 13 and 14. The ACAH response is clear. The nonlinear element was chosen to give a maximum pitch rate of 10 deg/s when the pilot demanded a large change in pitch attitude.

Table 3 Control gearings

Lateral stick X_A	0.2 rad/in.
Longitudinal stick X_B	0.1 rad/in.
Pedal X_c	0.17 rad/s/in.

Analysis of the data (e.g., Fig. 14) corresponding to a nose-down demand indicates that the control law was functioning exactly as intended. The pitch control law had been deliberately tuned to give a relatively low bandwidth in the belief that this would reduce the likelihood of stability problems. When it came to the flight test, the pitch axis was found to be sluggish and the evaluation pilot indicated that high-gain tasks would be difficult to perform, owing to the low bandwidth.

Several inputs were also used to excite the roll and yaw axes. Primary responses are displayed in Figs. 15 and 16. The desired ACAH and RC response types were achieved. The pilot described the roll axis response as crisp. From Fig. 16, one sees that the yaw rate

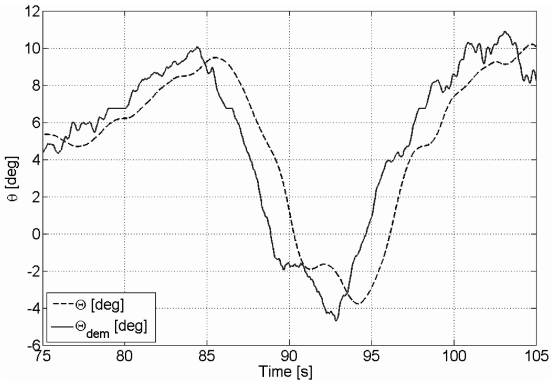

Fig. 13 Longitudinal inputs with FCL001 engaged.

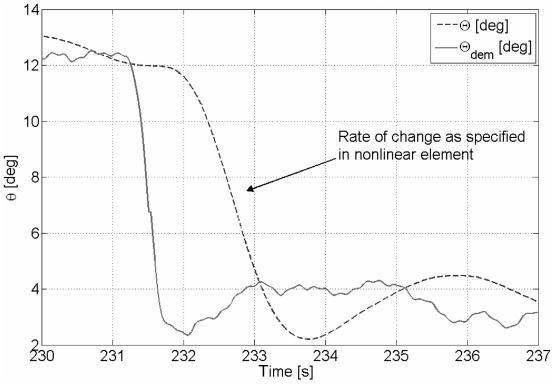

Fig. 14 Longitudinal step input with FCL001 engaged.

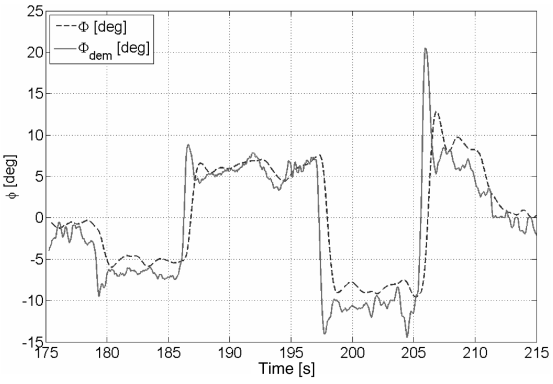

Fig. 15 Lateral inputs with FCL001 engaged.

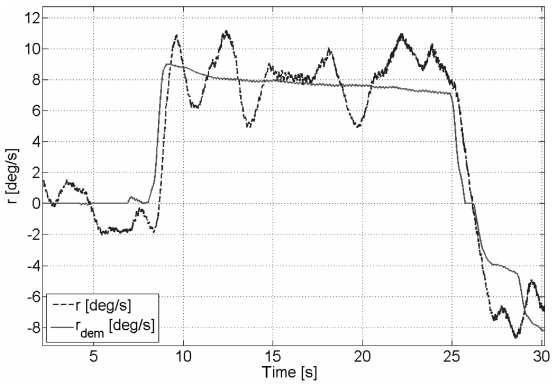

Fig. 16 Pedal inputs with FCL001 engaged.

tracked the reference signal in the mean, but that an oscillation was present that was evident to the pilot. This is thought to be the result of an interaction between the engine, governor, rotor speed, and yaw-axis dynamics. Excitation by wind gusts may also be a factor. Improvements may be achievable by closing a control loop around the heave axis.

Frequency sweeps were performed to determine the bandwidth of the closed-loop system in the roll and pitch axes. The bandwidths from the flight test and from calculations made on the 28-state linear model at the same flight condition are summarized in Table 4. The pitch bandwidth from the flight test was slightly higher than the prediction; this may be due to the fact that the pilot inputs in the flight test occasionally pushed the control law into the nonlinear regime, which would have made the gain of the outer loop increase, thereby increasing the bandwidth. The phase delay was underpredicted by the model for all three cases; prediction of phase delay relies on prediction of the phase characteristics of the closed-loop system at frequencies up to twice the bandwidth frequency, in which one would expect model fidelity to be lower. In addition, relatively simple Matlab-based routines were used to extract the frequency responses, and even though reasonable coherence was indicated, more sophisticated algorithms need to be investigated.

B. Flight Test of FCL002

The flight test of FCL002 took place in October 2006. The control gearings were identical to those in Table 3. Again, no stability problems were encountered when the controller was engaged. Most of the test was performed at around 20 kt. The pilot commented that the controller provided rock-solid control. Steplike and swept inputs were performed in the three axes. Primary responses to the steps are presented in Figs 17–19.

Reasonable tracking of the pitch and roll attitude was achieved. Tracking of the yaw rate was similar to that provided by FCL001, engine/drive train dynamics providing the most likely explanation for oscillatory behavior.

Frequency sweeps were performed in the three axes to determine the bandwidth and phase delay of the closed-loop system. The bandwidths and phase delays identified from this flight test are presented in Table 5 and are compared with the values predicted

Table 4 FCL001 bandwidths: flight test and 28-state linear prediction at 20 kt

Axis	ω_{BW}, rad/s	τ_p, s	Handling quality	
			Target acquisition and tracking MTEs	All other MTEs
Pitch, predicted	1.6	0.21	2	1
Pitch, flight test	1.8	0.37	3	1
Roll, predicted	3.7	0.06	1	1
Roll, flight test	3.8	0.12	1	1
Yaw, predicted	2.4	0.02	2	1
Yaw, flight test	2.4	0.05	2	1

Table 5 FCL002 bandwidths from flight test and from calculation on the 28-state linear model at 20 kt

Axis	ω_{BW}, rad/s	τ_p, s	Handling quality	
			Target acquisition and tracking MTEs	All other MTEs
Pitch, predicted	3.4	0.07	1	1
Pitch, flight test	3.5	0.19	1	1
Roll, predicted	3.6	0.07	1	1
Roll, flight test	3.5	0.15	2	1
Yaw, predicted	2.4	0.02	2	1
Yaw, flight test	2.6	0.15	2	1

using the 28-state linear model. Once again, the predicted and the achieved bandwidths correlate very well.

The safety pilot, for which the role was to monitor the control action taken by the FBW system in flight, commented that the control law behaved rather aggressively for large control inputs. The nonlinear element of FCL002 was therefore adjusted to use less

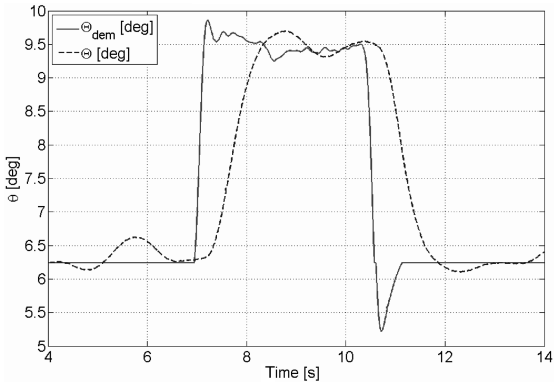

Fig. 17 Longitudinal inputs with FCL002 engaged.

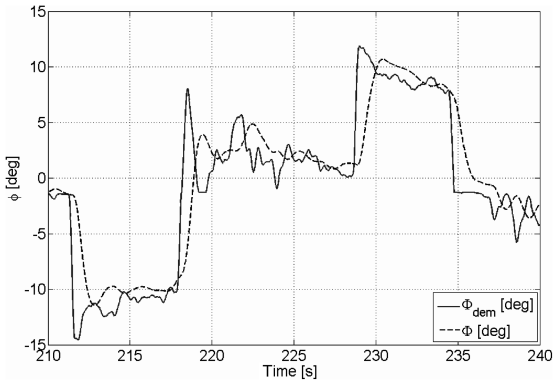

Fig. 18 Lateral inputs with FCL002 engaged.

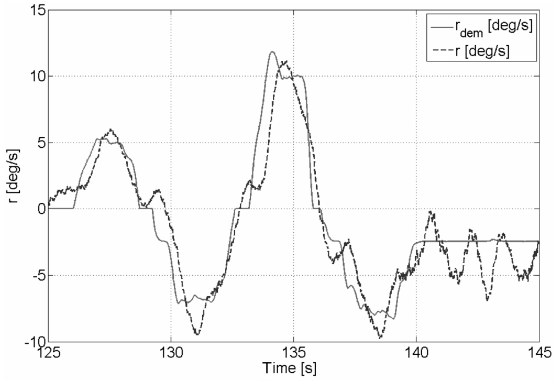

Fig. 19 Pedal inputs with FCL002 engaged.

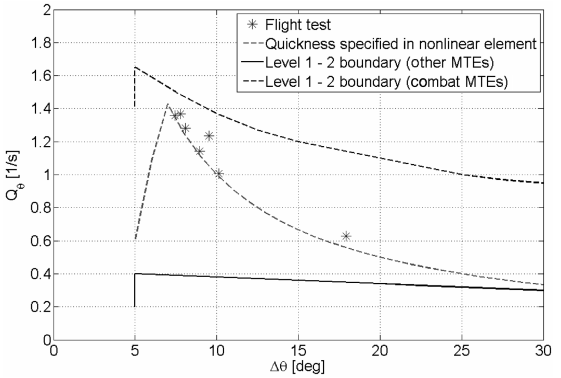

Fig. 20 FCL002B quickness in flight with rate of response set to 10 deg/s.

control authority by specifying a 10-deg/s speed of response. This modified version, designated FCL002B, was flight-tested in March 2007. Several large step inputs were conducted with the pitch controller to determine the quickness of the control law. Results of this test are presented in Fig. 20.

The quickness obtained in flight and that specified in the nonlinear element matched closely. The measured quickness is slightly higher than the specified level; this may be due to the fact that the inner loop has some overshoot, hence the peak pitch rate was slightly higher than demanded by the outer loop. The pitch attitude quickness was level 1 for all other mission task elements.

VII. Conclusions

Classical nonlinear control theory was used to design full-authority control laws giving a nonlinear ACAH response type. This can increase the agility of the system compared with a linear ACAH system. The method presented makes it possible for the designer to specify the speed of response of the system and thus the quickness. Two controllers were designed; the first (FCL001) was designed to investigate the use of a nonlinear outer feedback loop around a classical linear ACAH control law. Describing function analysis and the Popov criterion were used to predict the stability of the nonlinear control law. A slightly higher-performance variant of FCL001 was tested in the flight simulator at the University of Liverpool and comments from the pilot were very favorable; not only did the pilot know what attitude was commanded, but also what the corresponding rate would be. FCL001 was subsequently tested in flight and proved to be stable and flyable. The specified response type was achieved but the pitch axis was somewhat sluggish; the bandwidth was a relatively low 1.8 rad/s. A second controller (FCL002) was designed around a higher-performance linear RC inner loop. FCL002 also proved to be stable and flyable. The bandwidths achieved in flight matched the bandwidths predicted using the linear models developed in the project. Also, the pitch attitude quickness achieved in flight closely matched the attitude quickness specified in the nonlinear element. Overall, the use of a nonlinear element in this way appears to be an effective means of recovering some of the performance that is generally sacrificed when the level of augmentation is increased to ACAH. The testing of the control laws described in this paper was an important step in the HELIACT project. The models, design tools, and rapid prototyping setup are now in place and the plan now is to develop and test multi-objective control laws having load alleviation and envelope-protection functionality.

Acknowledgments

The research presented in this paper was funded by the Engineering and Physical Sciences Research Council under research grant GR/S42354/01. The authors are grateful to the anonymous reviewers for their help improving the paper.

References

[1] Gubbels, A. W., and Carignan, S. J. R. P., "NRC Bell 412 Advanced Systems Research Aircraft: A New Facility for Airborne Simulation," *Canadian Aeronautics and Space Journal*, Vol. 46, No. 2, June 2000, pp. 106–115.

[2] Baillie, S. W., Kereliuk, S., Murray Morgan J., and Hui, K., "Evaluation of the Dynamics and Handling Quality Characteristics of the Bell 412 HP Helicopter," *Canadian Aeronautics and Space Journal*, Vol. 40, No. 1, Mar. 1994, pp. 32–46.

[3] Manimala, B. J., Walker, D. J., Padfield, G. D., Voskuijl, M., and Gubbels, A. W., "Rotorcraft Simulation Modelling and Validation for Control Law Design," *The Aeronautical Journal*, Vol. 111, No. 1116, Feb. 2007, pp. 77–88.

[4] Walker, D. J., Manimala, B. J., Voskuijl, M., and Gubbels, A. W., "Multivariable Control of the Bell 412 Helicopter," *45th IEEE Conference on Decision and Control*, Inst. of Electrical and Electronics Engineers, Piscataway, NJ, 13–15 Dec. 2006, pp. 1527–1532.

[5] Stiles, R. L., Mayo, J., Freisner, A. L., Landis, K. H., and Kothmann, B. D., "Impossible to Resist: The Development of Rotorcraft Fly-by-Wire Technology," *Proceedings of the 60th annual forum of the American Helicopter Society*, AHS International, Alexandria, VA, 8–10 June 2004, pp. 1–18.

[6] Einthoven, P. G., Miller, J., Irwin, B., McCurdy, B., and Bender, J., "Development of Control Laws for the Chinook Digital AFCS Program," *Proceedings of the 62nd Annual Forum of the American Helicopter Society*, AHS International, Alexandria, VA, 9–11 May 2006.

[7] "Handling Qualities Requirements for Military Rotorcraft," *Aeronautical Design Standard*, U.S. Army Aviation and Missile Command, Aviation Engineering Directorate, Rept. ADS-33E-PRF, Redstone Arsenal, AL, 2000.

[8] Tischler, M. B., Blanken, C. L., Cheung, K. K., Swei, S. S. M., Sahasrabudhe, V., and Faynberg, A., "Modernized Control Laws for UH-60 BLACK HAWK Optimization and Flight-Test Results," *Journal of Guidance, Control, and Dynamics*, Vol. 28, No. 5, Sept.–Oct. 2005, pp. 964–978.

[9] Padfield, G. D., "Helicopter Flight Dynamics," Blackwell Science, Boston, 1996, p. 422.

[10] Gubbels, A. W., and Ellis, D. K., "NRC Bell 412 ASRA FBW Systems Description in ATA 100 Format," National Research Council of Canada, Institute for Aerospace Research, Rept. LTR FR-163, Ottawa, Canada, Apr. 2000.

[11] Du Val, R. W., "A Real-Time Multi-Body Dynamics Architecture for Rotorcraft Simulation," *The Challenge of Realistic Rotorcraft Simulation* [CD-ROM], Royal Aeronautical Society, London, 7–8 Nov. 2001.

[12] Peters, D. A., and He, C., "Finite State Induced Flow Models, 2: Three-Dimensional Rotor Disk," *Journal of Aircraft*, Vol. 32, No. 2, Mar.–Apr. 1995, pp. 323–333.

[13] Bailey, F. J., Jr., "A Simplified Theoretical Method of Determining the Characteristics of a Lifting Rotor in Forward Flight," NACA Rept. 716, 1941.

[14] Ingle, S. J., and Celi, R., "Effects Of Higher Order Dynamics on Helicopter Flight Control Law Design," *Journal of the American Helicopter Society*, Vol. 39, No. 3, July 1994, pp. 12–23.

[15] "Flight Control Systems: Design, Installation and Test of Piloted Aircraft, General Specification for," U.S. Air Force, Rept. MIL-F-9490D, June 1975.

[16] Panda, B., Mychalowycz, E., Kothmann, B., and Blackwell, R., "Active Controller for Comanche Air Resonance Stability Augmentation," *Proceedings of the 60th Annual Forum of the American Helicopter Society*, AHS International, Alexandria, VA, June 2004, pp. 2048–2059.

[17] Atherton, D. P., "Nonlinear Control Engineering," Van Nostrand Reinhold, New York, 1975.

[18] Popov, V. M., "Absolute Stability of Nonlinear Systems of Automatic Control," *Automation and Remote Control*, Vol. 22, No. 8, Mar. 1962, pp. 857–875.

[19] Padfield, G. D., and White, M. D., "Flight Simulation in Academia: HELIFLIGHT in its First Year of Operation at the University of Liverpool," *Aeronautical Journal*, Vol. 107, No. 1075, Sept. 2003, pp. 529–538.

[20] Padfield, G. D., "The Making of Helicopter Flying Qualities: A Requirements Perspective," *The Aeronautical Journal*, Vol. 102, No. 1018, Dec. 1998, pp. 409–437.

[21] Cooper, G. E., and Harper, R. P., "The Use of Pilot Ratings in the Evaluation of Aircraft Handling Qualities," NASA TN-D-5133, Apr. 1969.